JOURNAL OF GEOPHYSICAL RESEARCH, VOL. 88, PAGES 5657-5667, JULY 1, 1983

OBSERVATIONS OF CHARGING DYNAMICS

R. C. Olsen

Physics Department, University of Alabama in Huntsville, Huntsville, Alabama 35899

C. K. Purvis

NASA/Lewis Research Center Cleveland, Ohio

Plasma data from the UCSD Auroral Particles Experiments on Applied Technology Satellites 5 and 6 are used to investigate the dynamics of natural charging events. Both eclipse and daylight charging events are considered, and typical responses illustrated by data from specific events. Two different physical processes are found to be involved in the charging process. One of these is straightforward: the spacecraft structure potential responds rapidly to changes in the environment, typically changing by hundreds of volts in a few seconds. The other process is more subtle: differential charging and potential barrier formation precede structural charging and determines the time scale, typically tens of minutes are required for the potential to change by several hundreds of volts. The latter process is found to be predominately responsible for daylight charging on both spacecraft.

INTRODUCTION

Particle data from the University of California at San Diego (UCSD) Auroral Particles Experiments on Applied Technology Satellites (ATS) 5 and 6 have revealed a wide variety of effects related to the electrostatic charging of spacecraft in geosynchronous orbit. Charging of ATS 5 to negative kilovolt potentials in eclipse was first reported by DeForest [1972]. Subsequent reports have established that both ATS 5 and ATS 6 charged frequently to negative kilovolt potentials in eclipse [*DeForest,* 1973; *Goldstein and DeForest*, 1976; *Garrett et al.*, 1977], and to substantial negative potentials in sunlight [*DeForest*, 1973; *Reasoner et al*., 1976; *Johnson et al.*, 1978]. Observations of potential barriers on ATS 6 have been attributed to differential charging, i.e., to charging of some spacecraft surfaces to potentials more negative than that of the structure [*Whipple*, 1976, *Olsen et al.,* 1981]. These potential barriers change during daylight charging events, indicating that differential charging is increased during such events [*Johnson et al*., 1978]. Evidence of differential charging on ATS 5 has also been reported [*DeForest*, 1973]. The aspect of charging response which has not been discussed in the literature is the dynamics of natural charging events, meaning the time dependence of structural charging response and the temporal relationships between differential and structural charging. This aspect has been treated in the context of active charge control studies involving use of the ATS 5 hot wire filament electron emitter to alter the spacecraft's potential during eclipses [*Purvis and Bartlett*, 1980, *Olsen*, 1981]. In the active control studies, investigation of the dynamics provides the essential clue to understanding spacecraft response. The dynamics of natural charging events similarly provides clues leading to a fundamental understanding of spacecraft charging processes.

This paper describes the observed dynamics of natural charging events on the ATS spacecraft, illustrating their response with data from specific events. Because eclipse response is similar for the two spacecraft, data from one (ATS 6) are used to illustrate it. Data from both craft are shown for daylight charging events. This is an observations paper, and thus uses an empirical approach to investigate charging dynamics. The complementary analytical approach will be taken in a later paper [C. K. Purvis and R. C. Olsen, unpublished manuscript, 1983].

SPACECRAFT AND DETECTORS

The orbital configurations of ATS 5 and ATS 6 are sketched in figures 1 and 2 respectively, and some of the characteristics of the two spacecraft and the UCSD particles detectors are summarized in Table 1. The spacecraft configurations are discussed by *Purvis and Bartlett* [1980] and references therein. For present purposes it is difficult to note that they differ greatly in size, geometry and type of stabilization. Their single common feature is that the exteriors of both spacecraft are largely electrical insulators, so differential charging can occur on both craft.

The UCSD detectors on ATS 5 have been described in detail by *DeForest and Mcllwain* [1971]. Basically they consist of two pairs of electrostatic analyzers (ESA's) which detect electrons and ions with energies in the 50 eV to 50 KeV range in 64 steps with an energy resolution (AE/E) of 12%. About 20 seconds are required to scan the energy range. These detectors were fixed to the spacecraft body (see Figure 1) so that one pair views out from the cavity formed by the top solar array parallel to the spin axis, while the second pair looks radially outward. The spacecraft spin axis is nominally parallel to the earth's spin axis so the parallel detectors view approximately in the magnetic field direction.

The UCSD on ATS 6 have been described in detail by *Mauk and McIlwain* [1975]. They were an outgrowth of the ATS 5 detectors and are also ESA's detecting electrons and ions with energies 1 eV to 81 keV in 64 steps which could be scanned in 16 s. The main detectors were again arranged in two electron-ion pairs and were mounted on the Environmental Measurement Experiment (see Figure 2); one pair rotated in the north-south (NS) plane, and one in the east-west (EW) plane.

The time resolution with which charging dynamics can be observed with these instruments is clearly determined by the time required to complete an energy scan. The energy resolution is determined by the band pass of the ESA's. Because the width of the energy window increases with increasing energy, energy resolution is reduced when the spacecraft is charged.

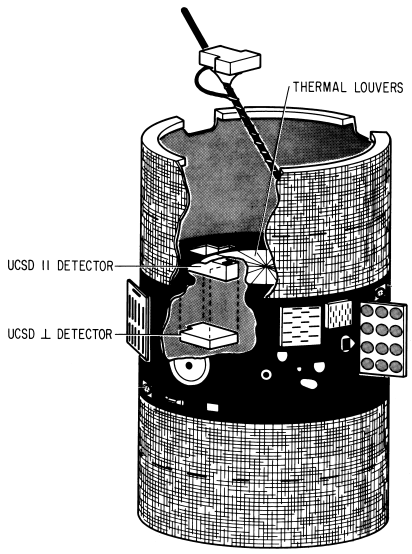

Fig. 1. ATS 5 spacecraft design. The spin stabilized satellite had its longitudinal axis oriented parallel to the earth's axis. The UCSD detectors looked parallel to the spin axis from inside the upper cavity, and radially outwards through the fiberglass belly band.

OBSERVATIONS OF CHARGING DYNAMICS

Information about two different aspects of the spacecraft's charge state can be obtained from the ESA data. One aspect is the potential of the structure or electrical reference with respect to the plasma at infinity. The other aspect is the existence of differential charging, i.e., the development of potentials different from the structure potential on various spacecraft surfaces. It is necessary to consider both aspects, and their interrelations, to obtain an understanding of dynamic charging response.

ATS 6 Eclipse Injection

It is well known that the largest negative potentials observed on the ATS 5 and ATS 6 spacecraft occurred during eclipse passage, and that abrupt changes in structure potential were frequently observed at eclipse entry and exit [*DeForest* 1972, 1973; *DeForest and Goldstein*, 1976; *Garrett and DeForest,* 1979]. Attempts to reproduce this behavior using simple probe theory and considering the effect of the penumbral passage in 'turning off' the solar photon flux [*Garrett and DeForest*, 1979] met with reasonable success for ATS 5, but were less successful for ATS 6. This was most probably related to the fact that ATS 6 was frequently charged tens to hundreds of volts negative potential before eclipse entry. Such precharging decidedly complicates the problem.

The simplest case of eclipse charging to analyze is that in which the spacecraft is initially at low potential (.6 10 V) in eclipse because the environment is quiet, and then an injection of hot plasma (a substorm) occurs, causing the 'spacecraft to charge negatively. There are a number of such cases in the ATS 6 data set. One occurred on October 2, 1975 (day 275) Particle data from the UCSD NS detector for this event are shown in spectrogram format in Figure 3. The spectrogram is an energy versus time plot for electrons (top) and ions (bottom), with the count rate of particles arriving at the detector indicated by intensity according to the grey scale to the right of the plot. Magnetic field components and detector look angle are indicated above the particle data (see *Mauk and McIlwain* [1975] for a more detailed description of the format). The data shown in Figure 3 were taken with the detector parked looking along the magnetic field (the pitch angle, a = 10° to 20°).

On October 2, 1975 ATS 6 entered eclipse at 2056 UT as determined by the solar array current. This is reflected in the particle data by the reduction in count rate of low energy electrons and the appearance of a low energy ion population. The low energy electrons in sunlight are spacecraft generated secondary and photoelectrons trapped by the positive spacecraft potential [*Olsen*, 1982]. The reduction in intensity of the electron flux is caused by the cessation of photoelectron production at eclipse entry and is a common feature in the ATS 6 data. The low energy ions are an ambient population which appear because of the slight shift in spacecraft structure potential from about 10 volts positive before eclipse to a few volts positive in eclipse. Such populations are a feature observed only during magnetically quiet periods [*Olsen,* 1982].

The injection process begins at about 2120 UT as signaled by the drop in intensity of the low energy ion flux and a small signal in the magnetometer data. With the appearance of the hot electrons the spacecraft charges rapidly to-about -6 kV as indicated by the change in the ion spectrum. The intense band of ions visible from the time of the injection to eclipse exit at 2202 UT is composed of low energy ions accelerated through the spacecraft's potential, and thus indicates the structure potential. The rise in 10- to 20-keV electron fluxes and the 5 kV drop in potential occur in less than 30 s, or 2 energy scan periods.

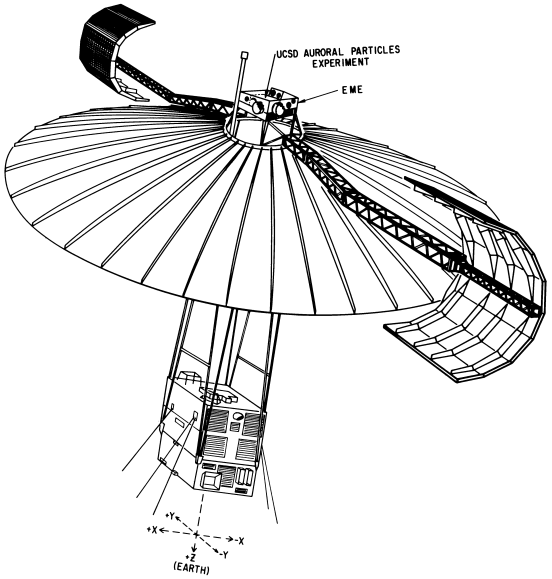

Fig. 2. ATS 6 spacecraft design and orientation. The three-axis stabilized spacecraft was oriented so that the large parabolic antenna was always pointed towards earth. The UCSD detectors are mounted on the Environmental Measurements Experiment package on the 'top' of the spacecraft, rotating in planes through and perpendicular to the earth's axis.

TABLE 1. Summary of Spacecraft Characteristics

	ATS 5	ATS 6
Launch date	1969	1974
Geometry	cylindrical	extended
Size	1.3 m diameter, 2 m long	16.5 m end to end (solar arrays)
Stabilization	spinning, 76 rpm	three-axis stabilized
Exterior surfaces	quartz, paint	kapton, quartz, silicon, paint, aluminum
UCSD detectors	body mounted, 50 eV to 50 keV	rotating, 1 eV to 81 keV

Subsequent to the injection, the energy of the environment drops, as indicated by the energy cutoff of the high energy electrons. There is a slight rise in energy at about 2128 UT which is followed by an essentially monotonic decline for the balance of the period shown in the spectrogram. The structure potential, as indicated by the ion data, exhibits a more complex behavior. After the initial rapid charging to about -6 kV, the structure potential becomes less negative, following the energy drop in the environment. However, the structure potential levels off at a few hundred volts negative between 2132 and 2134, and then becomes more negative again, reaching -2 kV by about 2145 and remaining essentially constant until eclipse exit. Three things about this second charging phase (2135 to 2145 UT) are notable. First, the spacecraft is not responding directly to a change in the environment. Second, the charging is very slow (5-10 min) compared to the response observed at injection (less than 1 min). Third, it is accompanied by the appearance of a substantial flux of low energy (20-40 eV) electrons whose energy-time profile seems to 'mirror' the structure potential change. This type of signature in the low energy electron data is a common feature in ATS 6 daylight charging events [*Johnson et al.,* 1978]. Examination of the electron distribution functions indicates that these low energy electrons are spacecraft generated [*Whipple* 1976a,b; *Olsen et al.,* 1981]. They therefore are secondary electrons returned by an electrostatic potential barrier caused by differential charging of some spacecraft surface with respect to the structure. The rise in energy of the returned electrons between their appearance at ~2134 UT and 2145 UT reflects an increase in the energy height of the potential barrier. This suggests a causal connection between the structural charging and the potential barrier. The barrier reduces the electron flux escaping from the spacecraft, and causes the spacecraft potential to become more negative. The long time constant for the charging response is consistent with this interpretation. The capacitance between an insulating surface and the underlying structure is much larger than the capacitance of the spacecraft as a whole to the plasma (at infinity). Therefore differential charging and structural charging driven by differential charging and consequent barrier formation are slow (see also *DeForest* [1973] and *Purvis and Bartlett* [1980].

At 2202 UT the spacecraft exited eclipse, and the structure potential became slightly positive. The banded structure in the ion data after eclipse exit is due to bouncing ion clusters [*Quinn and Mcllwain*, 1979] and is not related to charging effects.

To provide an indication of particle spectra capable of producing several kilovolt negative potentials in eclipse, the ion and electron count rates for 2125 UT are shown in Figures 4 and 5. At this time, the spacecraft frame potential was temporarily stable near -5 kV. The ion data from both the NS and EW detectors, shown in Figure 4, indicate that the parallel and perpendicular distributions are quite different. Both sets of data indicate the frame potential is -5.2 kV. The peaks in the count rates of ions with energy less than about 9 keV reflect the acceleration of lower energy ions through the spacecraft's potential. The count rate for perpendicular ions shows a peak at about 30 keV. Use of the fact that an ESA measuring a Maxwellian distribution shows a peak in the count rate at twice the temperature would suggest that these ions have a temperature of about 10-15 keV. This qualitative estimate should be used with great care, however. Close examination of the distribution functions for the ions (not shown) indicates that they are decidedly non-Maxwellian.

Figure 5 shows the parallel electron data. Data from the perpendicular detector are quite similar, indicating that the electrons are nearly isotropic. The data show a broad peak in the 10 to 15 keV region, with a smaller peak at 100 to 200 eV. A gain change occurred during the energy scan so that the count rates below 100 eV are magnified by a factor of 2 with respect to those at higher energies. The broad peak in count rate at 10-15 keV suggests a temperature of 5-10 keV for the electrons. Piecewise fits to the distribution functions (not shown) result in the following parameters: (1) 100-300 eV, noise or spacecraft generated; (2) 342-2000 eV, T_e = 2.0 keV, n_e = 0.765 cm^{-3}; (3) 2.1-54 keV, T_e = 6.7 keV, n_e = 0.422 cm^{-3}. These distributions are comparable to those found to charge ATS 5 to similar potentials in eclipse [*DeForest* 1972, 1973].

This event illustrates several typical features of eclipse charging response of both ATS 5 and ATS 6. Both spacecraft respond rapidly to environmental changes such as injection during eclipse and eclipse exit. Rapid charging on eclipse entry is also observed in substorm environments [*DeForest* 1972, 1973; *Goldstein and DeForest,* 1976]. In general, the structure potentials of both spacecraft tended to follow changes in the environment during eclipse. Structure charging responses associated with potential barrier formation during eclipse, such as occurred in this event (2135 to 2145 UT) are occasionally observed on ATS 6, but never on ATS 5.

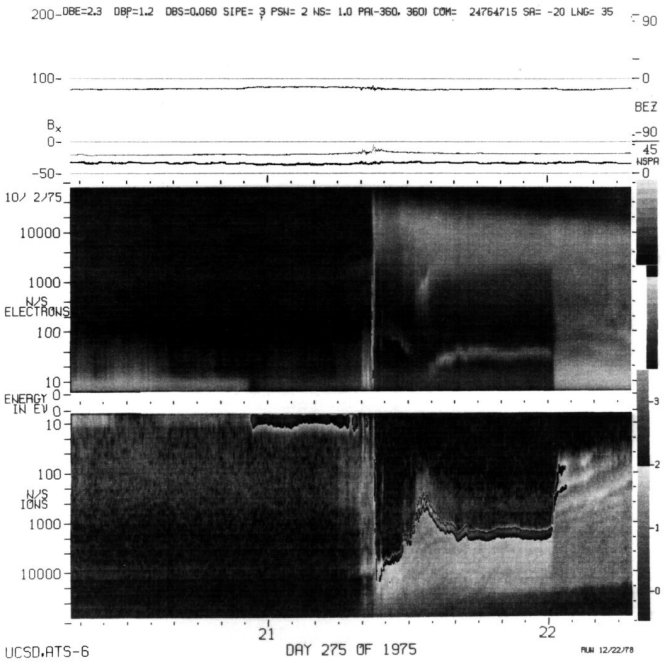

Fig. 3. ATS 6 spectrogram, October 2, 1975. An eclipse injection event occurs at 2122 UT, causing the spacecraft to charge to -6 kV. High ion fluxes in the 2 to 10 eV range cause the grey scale to cycle to black between 2057 and 2120 UT.

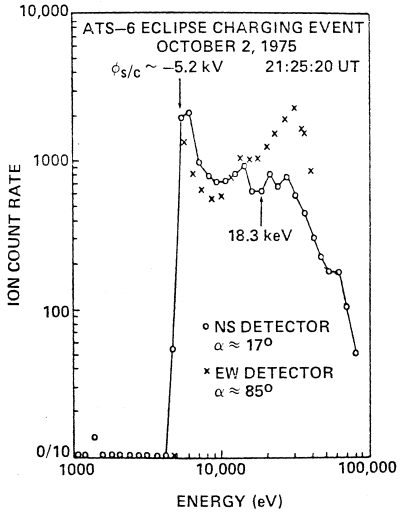

Fig. 4. Ion count rate, October 2, 1975, 2125:20 UT, local midnight. The count rates from the NS and EW detectors are shown. The spacecraft potential is about -5.2 kV.

ATS-6 Penumbral Eclipse

Eclipse passages are of great value because they provide a variation in one of the dominant terms in the spacecraft current balance, the photoelectron flux. From the standpoint of charging dynamics, the rate of spacecraft response to photocurrent changes is of particular interest. This is most easily seen by examining data from penumbral eclipses using the solar array current data as an indicator of spacecraft illumination.

A penumbral eclipse lasting from 0607:00 UT to 0622:30 UT occurred on September 5, 1974. Data from this event are shown in Figures 6 and 7. Figure 6 is a spectrogram of the eclipse period. An injection of hot plasma occurred about an hour before eclipse entry, and the energy of the environment was falling gradually. The spacecraft was charged slightly negative (-10 to -30 volts) before the eclipse began. The bright band of low energy electrons again indicates the presence of a potential barrier whose height varies between 20 and 40 volts as the detector assembly rotates. The diagonal line trace at the top of the figure indicates the pitch angle of the measured particles, reflecting the detector rotation. The ion data indicate a smooth variation in frame

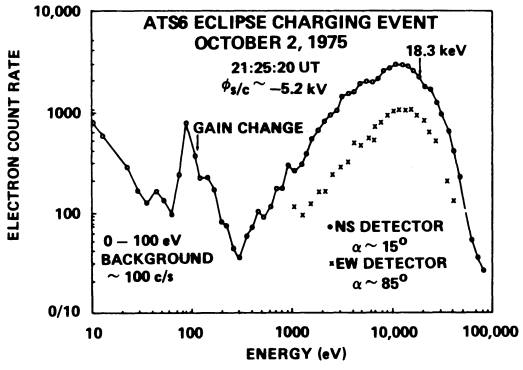

Fig. 5. Electron count rate, October 2, 1975, 2125:20 UT.

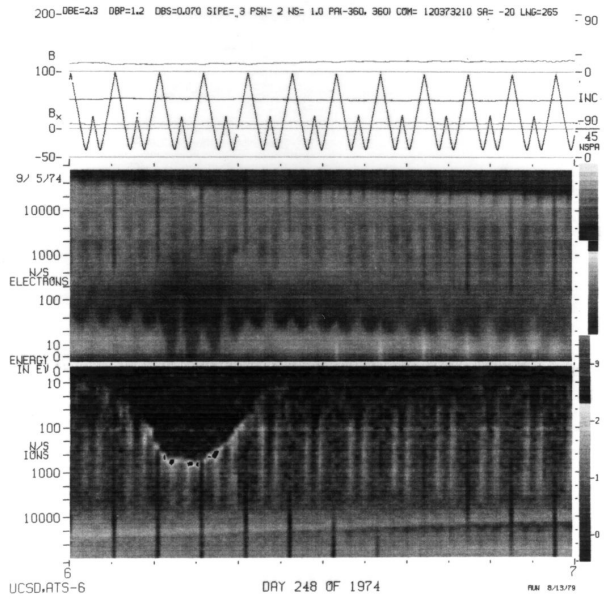

Fig. 6. ATS 6 spectrogram, September 5, 1974. A partial eclipse of the satellite is centered around 0615 UT, with the spacecraft potential and differential charging barrier height both dropping in the middle of the eclipse period. The rotation of the detector head is indicated by the diagonal pitch angle trace at the top of the spectrogram, and reflected in the angular structure of the differential charging barrier in the electron data, and the ambient ion data. Vertical light streaks in the ion data are field aligned ions, vertical black streaks in both species are the obstruction viewed by the detector at one end of the angular rotation.

potential during the eclipse. However, neither the potential variation or the changes in the barrier height seen in the electron data are symmetric about the midpoint of the eclipse at 0614:45 UT. The asymmetry is slight, but does suggest some difference between the entry and exit response characteristics.

Figure 7 shows a plot of solar illumination (as indicated by solar array current) versus frame potential, on a log-linear scale, for the eclipse entry and exit phases of this event. The asymmetry noted above is evident in this figure, particularly in the potential range -80 to -220 volts. Upon eclipse entry (x's in Figure 7), the frame potential changes slowly, falling from ~ -20 V to ~ -100 V as the array current drops from ~10 A to less than 2 A.

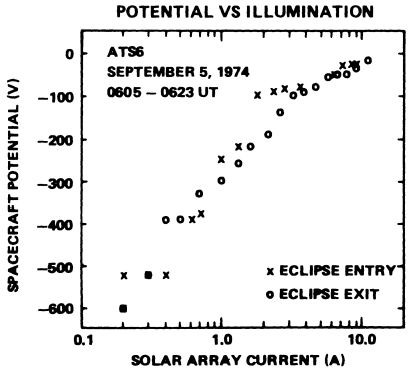

Fig. 7. ATS 6 potential plot, September 5, 1974. The spacecraft mainframe potential, as determined from the ion data, is plotted against the solar array current, which is proportional to the illumination of the spacecraft, and hence the photoelectric current.

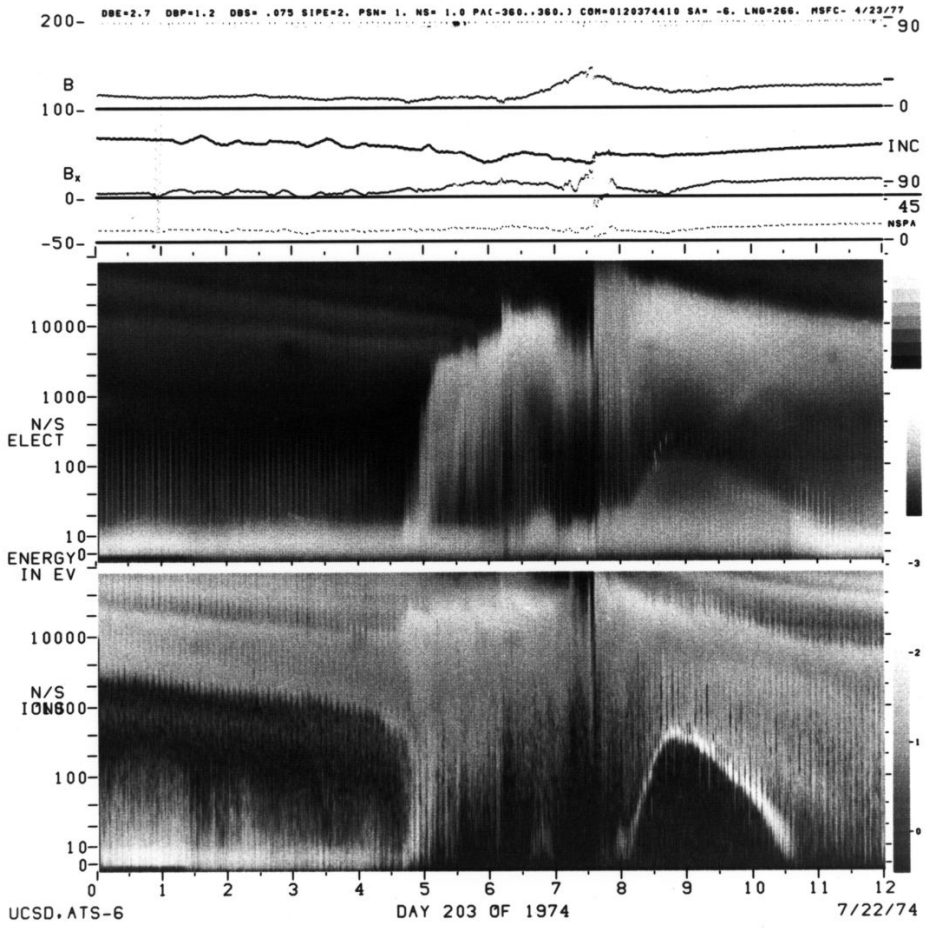

Fig. 8. ATS 6 spectrogram, July 22, 1974. A daylight charging event is shown here with data from the NS detectors featuring a single injection at 0735.

Then, as the array current is reduced from ~2 A to 1 A, the potential drops from -100 V to ~ -250 V and subsequently continues to fall rapidly with decreasing array current. The behavior during eclipse exit (circles in Figure 7) is much smoother, showing a near-linear dependence of potential on log (current) for potentials more negative than about -80 volts. Because photoelectrons and ambient electrons are the dominant sources of current to the spacecraft simple equilibrium spherical probe theory would predict such a linear dependence. Thus, for these potentials, the spacecraft potential is charging in direct response to changes in illumination. The response for potentials in the range -80 V to 0 V is not so straightforward. The fact that these potentials are comparable in magnitude to the potential barrier returning electrons to the spacecraft (several tens of volts) suggests that the barrier may be influencing the charging response for small magnitude potentials. The spacecraft is in the daylight charging regime at this point, as in the case described next.

ATS 6 Charging in Daylight

ATS 6 charged frequently in daylight to potentials as negative as -2 kV [*Reasoner et al.,* 1976]. The dynamics of daylight charging are most easily seen in events involving a single injection of hot plasma, as was the case for eclipse charging dynamics. Data from a single injection event on July 22, 1974 (day 203) are used here to illustrate daylight charging phenomena observed on ATS 6. Figure 8 shows the data in spectrogram format for hours 0000 to 1200 UT. The injection of hot plasma occurred at 0740 UT. A small amount of charging develops in response, but the charging does not really begin until 0800 UT. Examination of line plots at this time shows that at this the electron fluxes in the few hundred eV range drop. This would cause a drop in the secondary emission current from the spacecraft (*Olsen,* 1983). As in the previous examples, the energy of the environment, as indicated by the cutoff of high energy electrons, is first steady, then gradually decreasing, during the period shown in the spectrogram. The ion data indicate that the spacecraft structure potential falls gradually from 1-10 V at 0810 UT to nearly -400 V at 0840 UT, where it stabilizes briefly before commencing a slow rise back towards zero volts, which is

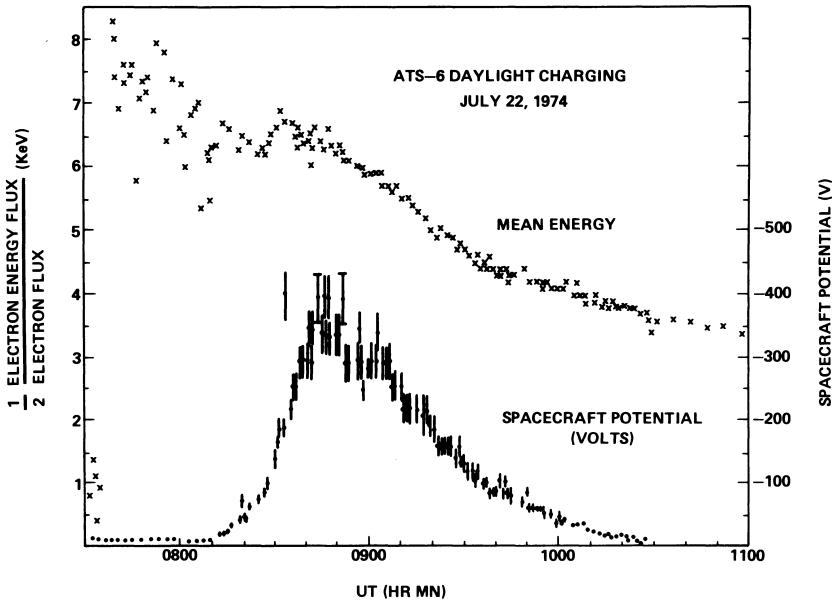

Fig. 9. ATS 6 potential plot, July 22, 1974. Mainframe potential and electron temperature are plotted throughout the charging event.

attained at 1040 UT. The upper energy cutoff of the bright band of low energy electrons changes during the charging sequence in a characteristic fashion. It rises as the structure charges negatively, reaches a maximum of about 150 V, and falls as the structure potential returns toward zero, appearing to mirror the charging signature in the ion data. As in the previous examples, these electrons are spacecraft generated, and returned to the detectors by a potential barrier. The energy height of the barrier is indicated by the energies of the returned electrons.

The charging of ATS 6 in response to this injection of hot plasma in daylight is strikingly different from its response to similar injections in eclipse. The most obvious difference is in the rate at which the spacecraft responds to the change in the environment. In eclipse, the spacecraft responded to the injection by charging to several kilovolts negative within one energy scan of the UCSD detectors (16 s). In daylight, 50 minutes were required for the spacecraft structure to reach its minimum potential of about -400 volts. There is no gradual increase in environmental energy to account for this long charging time. This can be clearly seen in Figure 9, where spacecraft structure potential and mean environment energy are plotted as functions of time for the daylight events. The mean energy used is the ratio of the third and first velocity moments of the electron distributions, divided by two. This is equal to the temperature for a Maxwellian distribution. The moments were obtained by numerical integration of the observed electron spectra, and are the same as those used by *Johnson et al.* [1978]. The choice of temperature as the significant plasma parameter is based on the linear relationship between potential and temperature from basic probe theory [*Whipple*, 1965]. It is evident from Figure 9 that the structural charging occurred during a period when the environment was relatively constant.

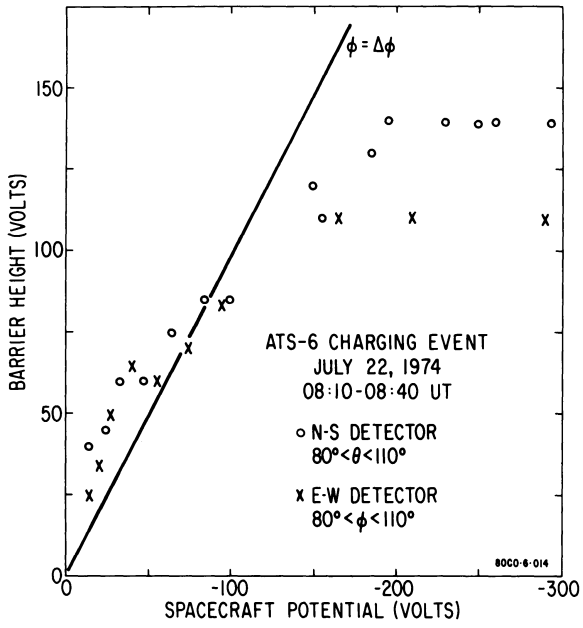

Fig. 10. ATS 6 potential plot, July 22, 1974. The mainframe potential and differential charging barrier height are plotted here for the event of Figures 8 and 9. The solid line labeled 4)_A4) is the barrier height equals absolute potential line, and shows the barrier height leads the potential initially, becoming equal at about 85 V at 0824 UT. The barrier height levels off shortly after 0830 UT, the EW detector at 110 V, the NS measurement at 130 to 140 V. This corresponds to the time when the exponential growth of the mainframe potential ends.

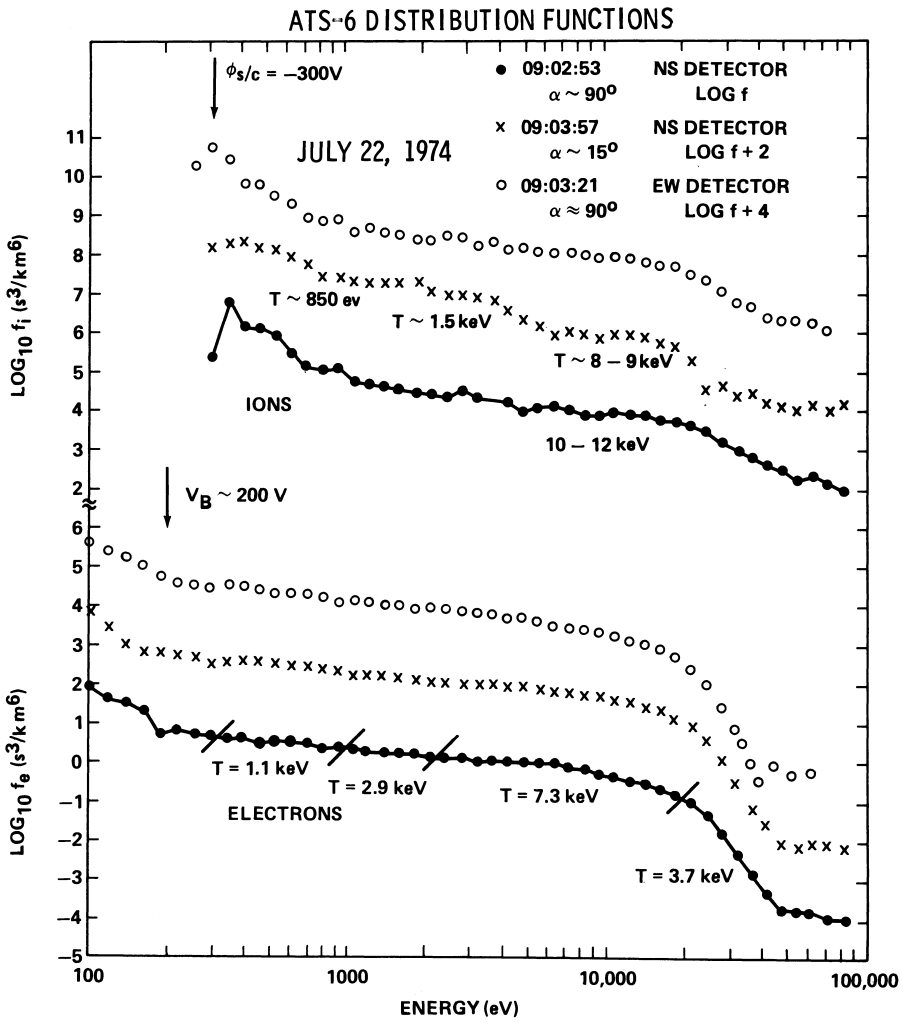

Fig. 11. ATS 6 distribution functions, July 22, 1974, 0930 UT, 0300 LT. Distribution functions for field-aligned and 90° ions and electrons are given as a function of energy. Note that a Maxwellian is not a straight line on a logarithmic energy scale. Spacecraft is charged to about -300 V, and an electrostatic barrier of about 200 V is visible in the electron data.

The structural charging here is not in direct response to an environmental change. The slow rise toward zero potential (0840 to 1040 UT), by contrast, follows the cooling of the environment rather closely (indeed, linearly), as would be predicted by simple probe theory. The long time constant of the charging from 0800 to 0840 UT requires an explanation different from direct response to environmental changes.

The clue to the physical process dominating the chargeup phase of this event lies in the relationship between the structure potential and the height of the potential barrier. The apparent mirroring of the structure potential in the low energy electron data which indicate the barrier height was noted earlier. Closer examination of the data reveals that this mirroring is rather imperfect. This can be seen from Figure 10, in which barrier height and structure potential are compared for the chargeup period. The barrier height leads the potential initially, reaching several tens of volts before any structural charging occurs. It then levels off at 100 to 150 volts while the structure continues to charge. The rate of structural charging increases after the barrier height has leveled off (see Figure 9).

The sequence of events which caused ATS 6 to charge on this day was evidently barrier formation followed by structural charging. Barrier formation is a consequence of differential charging [*Whipple*, 1976b, *Olsen et al.,* 1981], which is a slow process. This connects the long time constant for structural charging with differential charging.

Figure 11 shows the distribution functions taken by the NS detector (both field aligned and perpendicular) and the EW detector at 090253 UT, when the spacecraft potential was stable at -300 V. Electrons below 200 eV are electrons from the spacecraft surface, returned by the differential charging barrier [*Olsen et al*. 1981].

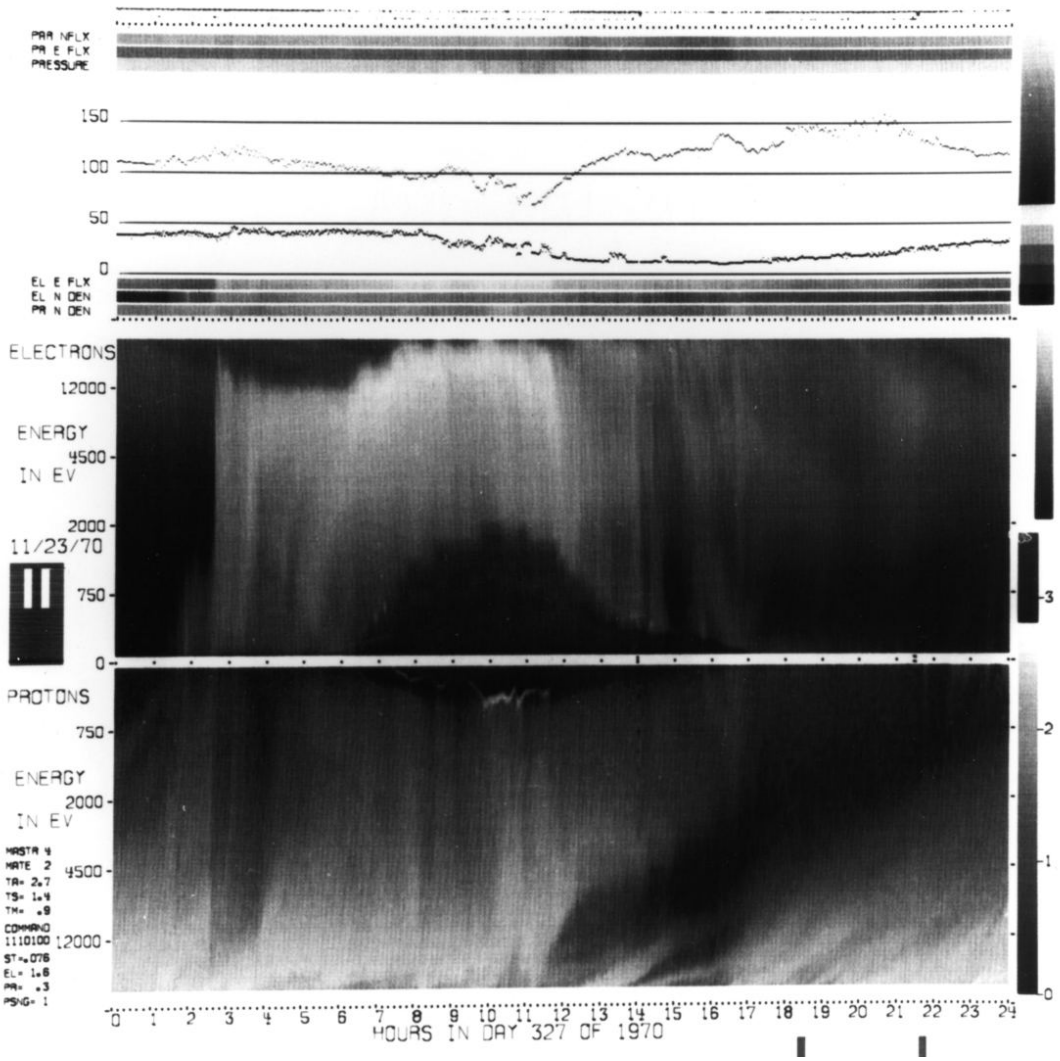

Fig. 12. ATS 5 spectrogram, November 23, 1970, parallel detector. Particle fluxes from 50 eV to 50 keV are shown here for 24 hours of ATS 5 operation. Charging effects are visible in the electron data from 0630 (local midnight) to almost 1700 UT. The beginning of the charging phenomena coincides with the appearance of electron fluxes above the 12 keV mark.

Ambient electrons below that energy are excluded by the differential charging barrier. Above the barrier, the electron distribution is nearly isotropic, and reasonably Maxwellian. The ion data are extremely anisotropic, and in no way Maxwellian. The low energy (500 to 6000 eV) ions are field aligned, while there is a loss cone above 25 keV. Temperatures were determined by piecewise least-square-fits to the distribution function.

The dominant part of the electron spectra is the 3 to 20 keV portion, which shows a 7.3 keV temperature, agreeing with the integrated value. The cooler plasma above the 25 keV transition point has a temperature of 3.7 keV, and is presumably the remains of an older plasma population which drifted around the earth [*DeForest and Mcllwain*, 1971] The ion distribution function is difficult to characterize, but the perpendicular population has a temperature of 10 to 12 keV, while the keV field aligned ions have a temperature of 8 to 9 keV. Note that this electron distribution, which resulted in a -300 V potential on ATS 6 in daylight, has a very similar temperature in the keV energy range to the one which was associated with a -5.2 kV potential on this same spacecraft in eclipse.

The charging response on this day is typical of ATS 6 daylight charging. This spacecraft frequently charged to several hundred volts negative in daylight; the record daylight potential was -2200 volts [*Reasoner et al*., 1976]. Daylight charging was always slow, and accompanied by potential barrier height changes similar to those seen in this event.

ATS 5 Daylight Charging

The initial observations of daylight charging on ATS 5 were made by DeForest [1972, 1973]. These observations were difficult to understand at that time, and were left unexplained. The insight gained from the ATS 6 daylight charging events into the importance of differential charging prompted a review

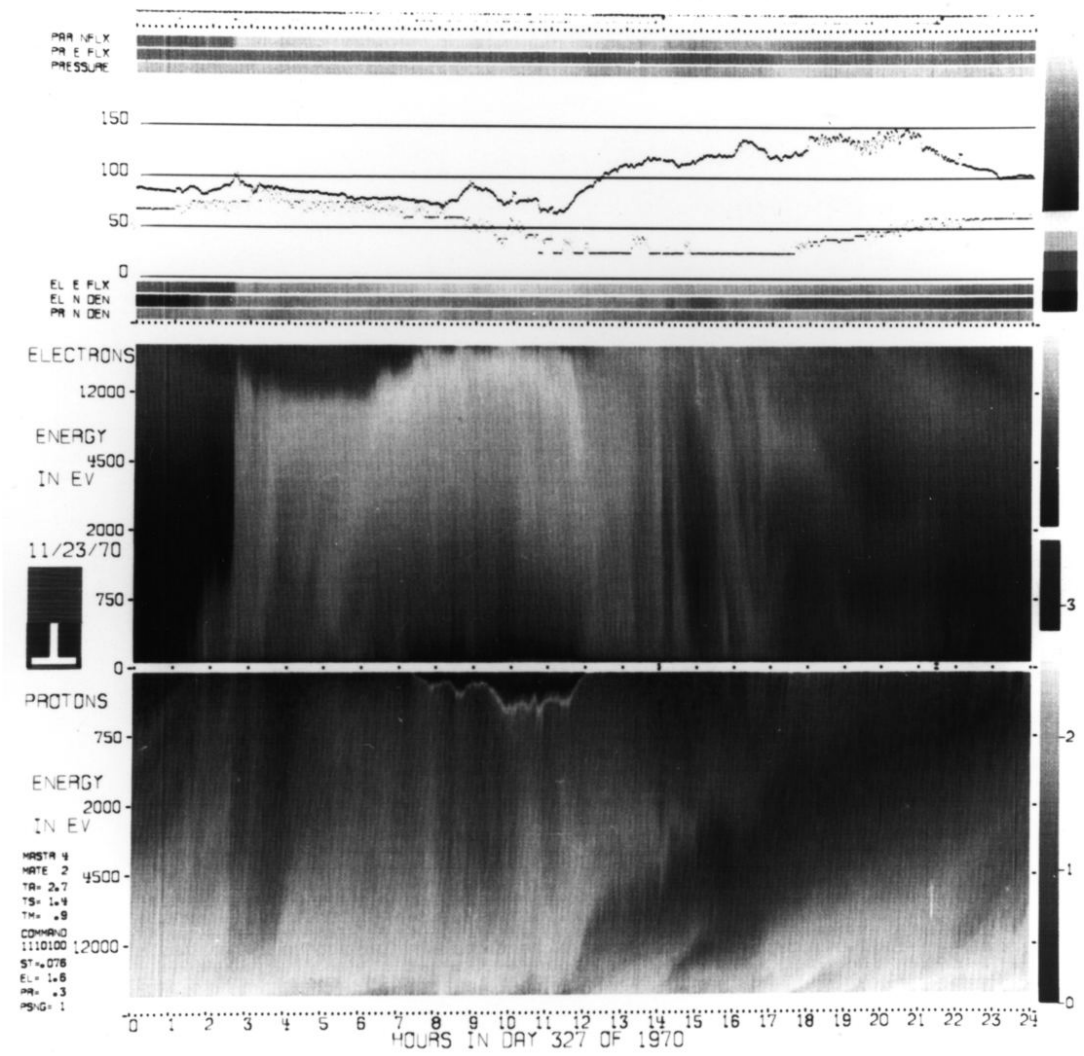

Fig. 13. ATS 5 spectrogram, November 23, 1970, perpendicular detector. Particle fluxes are from the detector which is looking radially away from the spacecraft do not show the contamination of electron data found in the cavity mounted parallel detector. A negative mainframe potential is shown by the ion data between 0700 and 1200 UT (midnight to dawn).

of ATS 5 data. As noted previously, ATS 5 and ATS 6 differed in size, geometry and type of stabilization. Yet they exhibited similar charging responses in eclipse. It therefore seems reasonable to seek evidence of differential charging associated with ATS 5 daylight charging events. Negative structure potentials are evidenced in the ion data in a similar fashion for both spacecraft, but the differential charging signatures are different.

Differential charging on ATS 5 is evidenced by a cutoff of the low energy electron data in the parallel detector. This cutoff was first identified as a charging effect by DeForest [1973]. In the review of ATS 5 data it was observed that daylight charging of this spacecraft was always preceded and accompanied by this signature in the low energy electron data taken by the parallel detector. Figure 12 shows data from this detector on November 23, 1970 (day 327). At about 0600 UT the environment gradually becomes more active; starting at about 0630 the cutoff of low energy electrons becomes evident as a reduction in the spectrogram's intensity. The energy of this cutoff rises slowly until about 1000, then gradually falls to zero by about 1200. The bright band of ions indicating spacecraft potential also appears in this data, but is more easily seen in the data from the perpendicular detector, which is not complicated by local charging effects in the cavity. The perpendicular detector data for this event is shown in Figure 13, again in spectrogram format. This figure shows that the spacecraft was charged to more than 50 V negative from about 0720 to 1200 on this day. The energy of the electron cutoff in the parallel detector and the spacecraft potential as determined from the perpendicular ion data are plotted on a linear scale in Figure 14 for the time period 0700 to 1200. By 0700, the electron energy cutoff was about 500 eV; it reached about 750 eV before the spacecraft potential reached -50 V.

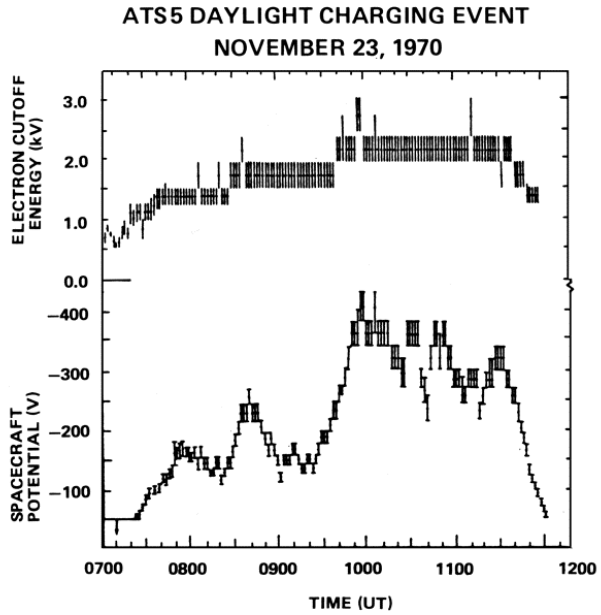

Fig. 14. ATS 5 potential plot, November 23, 1970. The spacecraft potential and electron cutoff energy are plotted against time for the event shown in the two previous figures. Error bars indicate channel width uncertainties.

The cutoff energy continued to increase as the spacecraft potential dropped, then began to fall off as the spacecraft potential rose to above -50 V at the end of the event. The most negative potential recorded was -390 V, around 1000 UT. Observations of a potential barrier evidenced by returned spacecraft-generated electrons have not been made for ATS 5, because the low energy detection cutoff of the detectors was 50 eV and the cavity mounted detector is shielded from photoelectrons generated on the outer body. In fact, anomalously high count rates in the lowest energy channels of the perpendicular detector occurred during a large portion of this charging event. This suggests that a barrier did exist, with a maximum energy height in the 50 to 80 eV range. Unfortunately, the enhanced count rates occupied so few energy channels that confident identification of their source is not possible.

This was one of the longest and most negative daylight charging events for ATS 5. Its basic characteristics, however, are typical. ATS 5 daylight charging events were always accompanied by differential charging in the cavity, and the magnitude of the differential potential was always larger than the mainframe potential. The mainframe never went more than 400 volts negative, and was typically -100 V, much more positive than typical ATS 6 values. ATS 5 also charged much less frequently than ATS 6. Nearly two years of data were reviewed, with only 46 daylight charging events found. [The statistical survey will be presented in a forthcoming paper by C. K. Purvis and R. C. Olsen (unpublished manuscript, 1983))

SUMMARY

Examination of eclipse and daylight charging responses of the ATS 5 and ATS 6 spacecraft with emphasis on temporal and environmental dependence has revealed that two basically different charging processes occur. In one process, the structure potential changes rapidly in response to changes in the environment. This was the process observed to dominate the charging response during eclipse injections, eclipse entry and exit, and the final phase of daylight charging events. The second process, which was found to dominate the early phase of daylight charging events, is more complex. It is invariably associated with differential charging and, on ATS 6, directly with potential barrier formation and growth. The fact that the barrier height leads the structure potential at the beginning of ATS 6 daylight charging events suggests that barrier formation with consequent suppression of low energy electron emission from the spacecraft is the dominant physical process in the early phases of daylight charging events. While no direct observations of barrier formation can be made confidently for ATS 5, the observation that differential charging is always associated with daylight charging events suggests that the basic mechanism is the same for both spacecraft.

ATS 5 and ATS 6 charged to similar potentials with similar frequencies in eclipse. By contrast, ATS 6 charged much more frequently and to larger negative potentials in daylight than did ATS 5. This is consistent in principle with the two different charging processes postulated here. Eclipse charging response is in general of the type in where the spacecraft structure potential is responding directly to environmental changes. Daylight charging evidently requires formation of potential barriers to suppress photoelectron emission. The latter process is expected to be far more dependent on spacecraft configuration (geometry, stabilization, size) than the former. Therefore similar charging responses in eclipse and different ones in daylight for ATS 5 and ATS 6 are quite reasonable. It may also be noted that the observations presented herein suggest that a spacecraft with no insulating surfaces, and therefore no differential charging, is expected never to experience daylight charging, but to charge in eclipse. This is consistent with the data from the GEOS spacecraft [J. F. E. Johnson, private communication, 1981].

Further examination of the relationships among differential charging, barrier formation and structural charging, and their dependence on spacecraft configuration is most easily accomplished via an analytical approach. This is the subject of a forthcoming paper by C. K. Purvis and R. C. Olsen.

Acknowledgements. This research was supported by the National Aeronautics and Space Administration under contracts NAS8-33982 and NSG-3150. The authors wish to thank S. E. DeForest and C. E. McIlwain for the ATS 5 and ATS 6 data, respectively. We would also like to thank N. J. Stevens for his comments and suggestions.

The editor thanks E. C. Whipple and A. Rubin for their assistance in evaluating this paper.

REFERENCES

DeForest, S.E., Spacecraft charging at synchronous orbit, *J. Geophys. Res*., 77, 651-659, 1972.

DeForest, S. E., Electrostatic potentials developed by ATS 5, in Photon and Particle Interactions with Surfaces in Space, edited by R. J. L. Grard, pp. 263-276, D. Reidel Pub., Hingham, Mass., 1973.

DeForest, S. E., and C. E. Mcllwain, Plasma clouds in the magnetosphere, *J. Geophys. Res*., 76, 3587-3611, 1971.

Garret, H. B., and S. E. DeForest, Time-varying photoelectron flux effects on spacecraft potential at geosynchronous orbit, *J. Geophys. Res*., 84, 2083-2088, 1979.

Garrett, H. B., A. L. Pavel, and D. A. Hardy, Rapid Variations in Spacecraft Potential, Air Force Surveys in Geophysics, 369, AFGL-TR-77-0132, 1977.

Goldstein, R., and S. E. DeForest, Active control of spacecraft potentials at geosynchronous orbit, in Spacecraft Charging by Magnetospheric Plasmas, Progress in Aeronautics and Astronautics, 47, edited by A. Rosen, pp. 169-181, AIAA, New York, 1976.

Johnson, B., J. Quinn, and S. DeForest, Spacecraft Charging on ATS 6, in Effect of the Ionosphere on Space and Terrestrial Systems, edited by J. Goodman, pp. 322-327, U.S. GPO, Washington D.C., 1978.

Mauk, B. H., and C. E. Mcllwain, ATS-6 UCSD auroral particles experiment*, IEEE Trans. Aerosp. Electron. Syst.,* AES-11, 1125-1130, 1975.

Olsen, R. C., Modification of spacecraft potentials by electron emission on ATS 5*, J. Spacec. Rockets*, 18, 527-532, 1981.

Olsen, R. C., The hidden ion population of the magnetosphere, *J. Geophys. Res*., 87, 3481-3488, 1982.

Olsen, R.C., A threshold effect for spacecraft charging, *J. Geophys. Res*., 88, 493-499, 1983.

Olsen, R. C., C. E. Mcllwain, and E. C. Whipple, Observations of differential charging effects on ATS 6, *J. Geophys. Res*., 86, 6809-6819, 1981.

Purvis, C. K., and R. O. Bartlett, Active control of spacecraft charging, in Space Systems and Their Interactions with Earth's Space Environment, Progress in Aeronautics and Astronautics, 71, edited by H. B. Garret, C. D. Pike, pp. 299-317, AIAA, New York, 1980.

Quinn, J., and C. E. Mcllwain, Bouncing Ion clusters, *J. Geophys. Res*., 84, 7365-7370, 1979.

Reasoner, D. L., W. Lennartsson, and C. R. Chappell, Relationship between ATS 6 spacecraft-charging occurrences and warm plasma encounters, in Spacecraft Charging by Magnetospheric Plasmas, 47, edited by A. Rosen, pp. 89-101, AIAA, New York, 1976.

Whipple, E. C. Jr., The equilibrium electric potential of a body in the upper atmosphere and in interplanetary space, Ph.D., thesis, George Washington University, Washington, D.C., NASA Tech. Note X-615-65-296, 1965.

Whipple, E. C. Jr., Theory of the spherically symmetric photoelectron sheath: A thick sheath approximation and comparison with the ATS 6 observation of a potential barrier, *J. Geophys. Res*., 81, 601, 1976a.

Whipple, E. C. Jr., Observation of photoelectrons and secondary electrons reflected from a potential barrier in the vicinity of ATS 6, *J. Geophys. Res*., 81, 715, 1976b.